



Heriot-Watt University  
Research Gateway

# Ceria promoted deoxygenation and denitrogenation of *Thalassiosira weissflogi* and its model compounds by catalytic in-situ pyrolysis

## Citation for published version:

Aysu, T, Maroto-Valer, MM & Sanna, A 2016, 'Ceria promoted deoxygenation and denitrogenation of *Thalassiosira weissflogi* and its model compounds by catalytic in-situ pyrolysis', *Bioresource Technology*, vol. 208, pp. 140-148. <https://doi.org/10.1016/j.biortech.2016.02.050>

## Digital Object Identifier (DOI):

[10.1016/j.biortech.2016.02.050](https://doi.org/10.1016/j.biortech.2016.02.050)

## Link:

[Link to publication record in Heriot-Watt Research Portal](#)

## Document Version:

Peer reviewed version

## Published In:

Bioresource Technology

## General rights

Copyright for the publications made accessible via Heriot-Watt Research Portal is retained by the author(s) and / or other copyright owners and it is a condition of accessing these publications that users recognise and abide by the legal requirements associated with these rights.

## Take down policy

Heriot-Watt University has made every reasonable effort to ensure that the content in Heriot-Watt Research Portal complies with UK legislation. If you believe that the public display of this file breaches copyright please contact [open.access@hw.ac.uk](mailto:open.access@hw.ac.uk) providing details, and we will remove access to the work immediately and investigate your claim.

## Accepted Manuscript

Ceria promoted deoxygenation and denitrogenation of *Thalassiosira weissflogi* and its model compounds by catalytic in-situ pyrolysis

Tevfik Aysu, M.M. Maroto-Valer, Aimaro Sanna

PII: S0960-8524(16)30183-3

DOI: <http://dx.doi.org/10.1016/j.biortech.2016.02.050>

Reference: BITE 16100

To appear in: *Bioresource Technology*

Received Date: 21 December 2015

Revised Date: 10 February 2016

Accepted Date: 11 February 2016

Please cite this article as: Aysu, T., Maroto-Valer, M.M., Sanna, A., Ceria promoted deoxygenation and denitrogenation of *Thalassiosira weissflogi* and its model compounds by catalytic in-situ pyrolysis, *Bioresource Technology* (2016), doi: <http://dx.doi.org/10.1016/j.biortech.2016.02.050>

This is a PDF file of an unedited manuscript that has been accepted for publication. As a service to our customers we are providing this early version of the manuscript. The manuscript will undergo copyediting, typesetting, and review of the resulting proof before it is published in its final form. Please note that during the production process errors may be discovered which could affect the content, and all legal disclaimers that apply to the journal pertain.



**Ceria promoted deoxygenation and denitrogenation of *Thalassiosira weissflogi* and its model compounds by catalytic in-situ pyrolysis**

**Tevfik Aysu<sup>a,b</sup>, M.M. Maroto-Valer<sup>a</sup>, Aimaro Sanna<sup>a\*</sup>**

<sup>a</sup> *Institute of Mechanical, Process and Energy Engineering School of Engineering and Physical Sciences, Heriot-Watt University, EH14 4AS, Edinburgh, UK*

<sup>b</sup> *Department of Chemistry, Faculty of Education, Yuzuncu Yil University, 65080, Van, Turkey.*

\* *Corresponding Author: [A.Sanna@hw.ac.uk](mailto:A.Sanna@hw.ac.uk)*

**ABSTRACT**

Pyrolysis of microcrystalline cellulose, egg white powder, palm-jojoba oils mixtures *Thalassiosira weissflogi* model compounds was performed with CeO<sub>2</sub> at 500°C, to evaluate its catalytic upgrading mechanism. Light organics, aromatics and aliphatics were originated from carbohydrates, proteins and lipids, respectively. Dehydration and decarboxylation were the main reactions involved in the algae and model compounds deoxygenation, while nitrogen was removed as NH<sub>3</sub> and HCN. CeO<sub>2</sub> increased decarbonylation reactions compared to in absence of catalyst, with production of ketones. The results showed that the catalysts had a significant effect on the pyrolysis products composition of *Thalassiosira weissflogi*. CeO<sub>2</sub>, NiCeAl<sub>2</sub>O<sub>3</sub> and MgCe/Al<sub>2</sub>O<sub>3</sub> catalysts increased the aliphatics and decreased the oxygen content in bio-oils to 6-7 wt% of the algae starting O<sub>2</sub> content. Ceria catalysts were also able to consistently reduce the N-content in the bio-oil to 20-38% of that in the parent material, with NiCe/Al<sub>2</sub>O<sub>3</sub> being the most effective.

*Keywords:* Catalytic pyrolysis, Bio-oil, *Thalassiosira weissflogi*, Model compound, Ceria.

## 1. Introduction

Fossil fuels currently provide the majority of our energy and chemical needs. However, fossil fuels are limited, unsustainable and have a negative impact on the environment. Biomass has attracted worldwide attention as renewable source for fossil fuels replacement. Algae or microalgae represent a promising alternative renewable source since they can be cultivated on non-arable land and recycle nutrients from waste water and flue-gas, and thus providing additional environmental benefits. The potential of microalgae as feedstock has already been investigated (Vardon et al., 2015; Costanzo et al., 2015). Compared to lignocellulosic biomass, microalgae have high photosynthetic efficiency, high productivity, high lipid (up to 80%) content and do not compete with food crops (Maguyon et al., 2013). In recent years, high-lipid microalgae species have received increasing attention for biodiesel production.

However, the extraction of oil from algae has higher costs compared to vegetable oils, due to the intrinsic different algae physico-chemical properties, such as cell size and cell wall chemistry. Furthermore, algae biodiesel has certain disadvantages, such as a high cloud point and low energy content that limit its wider usage (Gerpen JV, 2005). Another problem with algal biodiesel is that only the lipid portion of algae is utilized and the rest (carbohydrates and proteins) is considered as waste in terms of fuel use (Na et al., 2012). For low-lipid microalgae, thermochemical conversion processes such pyrolysis for conversion of all components is more suitable to produce bio-fuels or valuable chemicals (Vardon et al., 2015; Wang et al., 2013). Among thermochemical processes, pyrolysis has received growing attention in conversion of whole microalgae due to its relatively low cost and flexibility.

Pyrolysis bio-oil can be used as feedstock for value-added chemicals such as resins, adhesives and phenols or can be used as liquid fuel (Abdullah et al., 2008; Trinh et al., 2013).

Although microalgae to biodiesel has been studied extensively, microalgae catalytic pyrolysis has received less attention, with studies mainly focusing on the effect of the process variables

using acid zeolites, which tend to favour dehydration reactions and formation of aromatics products (Gopakumar et al., 2012). Microalgae have a very different chemical composition from wood and other lignocellulosic feedstocks. Hence, bio-oil produced from pyrolysis of microalgae contains a variety of different compounds, such as oxygenates, linear hydrocarbons and nitrogenous species resulting from pyrolysis of lipids and proteins, respectively. In principle, these differences from lignocellulosic feedstocks may lead to improved properties in the resulting bio-oil, such as higher heating values and reduced tar formation. Since microalgae contain carbohydrate, protein, and lipid as their main components, they devolatilize relatively at lower temperatures than lignocellulosic biomass materials (Peng et al., 2001). Furthermore, the bio-oil produced from microalgae is generally more stable due to lower O/C ratio, less acidic and has higher HHV compared to lignocellulosic bio-oil (Fisk et al., 2009). However, to date, there have been a limited number of studies on the pyrolytic characteristics of algae and their components. Since the heterogeneous composition of the different bio-feedstock affects the selection of the catalysts, process conditions and products yield and quality, catalysts that are effective in converting lignocellulosic biomass may not perform well with marine biomasses. For example, alumina supported Ni-based catalysts have been used in pyrolysis–gasification of freshwater algae to produce H<sub>2</sub> rich gases. Ni-based catalyst activated the cracking and reforming of biomass volatiles and tars released during pyrolysis at low temperatures (Díaz-Rey et al., 2014). Most of the previous studies on catalytic conversion of biomass (lignocellulosic and algal) have been primarily focused on the effects of process variables on the quality and quantity of bio-oil. Few reports on pyrolysis mechanism of biomass components have been reported (Du et al., 2013; Gai et al., 2015; Wang et al., 2014). Therefore, there are significant knowledge gaps on catalytic upgrading mechanisms using different catalysts that can favour the removal of O<sub>2</sub> from in-situ biomass decarboxylation and may selectively favour desired products.

In our previous study (Aysu and Sanna, 2015), we have evaluated the influence of ceria based alumina and zirconia supported catalysts on pyrolysis product yields and bio-oil properties of relatively high lipid containing alga, *Nannochloropsis*. However, there is no comparative study regarding the effect of ceria based catalysts on pyrolysis of low lipid algae such as *Thalassiosira weissflogi* and a lack of studies on the effect of ceria catalysts on microalgae model compounds pyrolysis. Therefore, the objectives of this study were: (i) to evaluate the effect of temperature and alumina supported ceria catalysts on product yields and the distribution of pyrolytic products using  $^1\text{H-NMR}$ , EA, TGA and GC-MS, (ii) to evaluate the mechanisms involved in the in-situ catalytic upgrading of the algae major components (proteins, fatty acids and carbohydrates), by conducting pyrolysis of model compounds using gas analysis and GC-MS.

## 2. Materials and Methods

### 2.1 Feedstock pre-treatment

The microalgae sample, *Thalassiosira weissflogi* was obtained from Varicon Aqua Solutions in liquid form. The algae cells were dried in an oven at 50 °C, pulverized to a particle size between 80 and 140 meshes (105-174  $\mu\text{m}$ ) and stored in a desiccator for further use. Micro-crystalline cellulose, dried egg whites (mixture of albumins, mucoproteins and globulins) and fatty acids (mixture of 70% palm oil (rich in C16:1) and 30% jojoba oil (rich in C20:1 and C22-2)) were used as model compounds of carbohydrates, proteins and lipids, respectively.

### 2.2. Catalyst preparation and characterization

Commercial ceria ( $\text{CeO}_2$ ) nanopowder was purchased from Sigma-Aldrich. Ceria containing catalysts ( $\text{Ce/Al}_2\text{O}_3$ ,  $\text{NiCe/Al}_2\text{O}_3$ ,  $\text{MgCe/Al}_2\text{O}_3$ ) were prepared by incipient wet impregnation method with  $\text{Ce}(\text{NO}_3)_3 \cdot 6\text{H}_2\text{O}$ ,  $\text{Mg}(\text{NO}_3)_2 \cdot 6\text{H}_2\text{O}$ ,  $\text{Ni}(\text{NO}_3)_2 \cdot 6\text{H}_2\text{O}$  as precursors using alumina support. The preparation method has been previously described (Aysu and Sanna, 2015). The  $\text{Ce/Al}_2\text{O}_3$  catalyst preparation was carried out by stirring cerium (III) nitrate

solution and alumina support at 300 rpm for 3 h at 80 °C. Then, the mixture was dried at 110 °C for 24 h. The dried  $\text{Ce}(\text{NO}_3)_2/\text{Al}_2\text{O}_3$  was calcined in air at 600 °C for 3 h to obtain a theoretical 5%  $\text{Ce}/\text{Al}_2\text{O}_3$  and to achieve well dispersion (Ying et al., 2012). The  $\text{Ce-Ni}/\text{Al}_2\text{O}_3$  catalyst was prepared by wet impregnating alumina with the cerium (III) nitrate solution and nickel (III) nitrate solution. The other catalysts were prepared using the same impregnation/calcination method described above. The surface area, pore volume and average pore size of the prepared catalysts were analyzed by  $\text{N}_2$  adsorption method at -195.8 °C using Micromeritics Gemini VII instrument. The catalyst samples were outgassed overnight at 180 °C. The surface area and pore size distribution of the samples were calculated by using the standard Brunauer–Emmett–Teller (BET) equation and the Barrett–Joyner–Halenda (BJH) method, respectively. The crystalline phases of the catalysts were identified by powder X-ray diffraction using Bruker D8 Advance powder diffractometer, operating with Ge-monochromated  $\text{Cu } K\alpha_1$  radiation (wavelength=1.5406 Å, 40 kV, 30 mA) and a LynxEye linear detector in reflectance mode. Data were collected over the angular range 5°-85° degrees in two-theta under atmospheric pressure.

### 2.3. Feedstock and products analyses

#### 2.3.1. Proximate and ultimate analysis

The moisture content and proximate analysis (volatile matter and ash content) of the dried *Thalassiosira weissflogi*, bio-oils and bio-chars were determined according to ASTM standards (D2016, E872-82, D1102-84). The carbon, hydrogen and nitrogen contents of dried *Thalassiosira weissflogi* and model compounds bio-oils and bio-chars were determined using Exeter Analytical CE440 analyzer and the oxygen content was calculated by difference.

Higher heating values (HHV) of samples were calculated by using Dulong's Formula as shown in Eq. (1), based on the elemental composition.

$$\text{HHV (MJ/kg)} = 0.3383 * \text{C} + 1.422 * (\text{H-O}/8) \quad (1)$$

where C, H, and O represent the weight percentages of carbon, hydrogen, and oxygen, respectively (Aysu, 2015).

### 2.3.2. $^1\text{H}$ NMR analysis

The  $^1\text{H}$  NMR analyses of *Thalassiosira weissflogi* and model compounds bio-oils were performed using Bruker Avance III operating at 400 MHz. The samples were prepared in  $\text{CDCl}_3$  with the ratio of 1:1 by volume in 5 mm NMR tube and using TMS (tetramethylsilane) as the internal standard.

### 2.3.3. TGA analysis

Thermogravimetric analysis was carried out using a TA Q500 thermogravimetric analyzer. TG-pyrolysis using  $\text{N}_2$  as carrier gas was used to determine the moisture content, volatile matter and fixed carbon and to compare/confirm with the results obtained by ASTM standards. TG-combustion using air as carrier gas was used to determine the ash content. The samples, weighing approximately 10 mg, were heated from 25 to 800 °C with a constant heating rate of 20°C/min under  $\text{N}_2$  and then the temperature was decreased to 600°C to determine the fixed carbon and ash contents under air atmosphere. The loss of weight between 25 and 105 °C was used to calculate the moisture content of the samples. The volatile content of the raw material was determined from the weight loss between 105 and 600°C as primary volatiles and 600 and 800 °C as secondary volatiles. The ash content of the sample was determined from the amount of solid remaining at the end of the combustion step. Fixed carbon was calculated by subtracting the ash content from the solids remaining at the end of run. The volatile contents of the bio-oils were determined from the weight loss between 25 and 105°C as light volatiles, and 105 and 600°C as heavy volatiles.

### 2.3.4. GC-MS and gas analysis

Agilent GC-MS 7890A/5975C series (Agilent Technologies, Santa Clara, CA) was used for the semi-quantitative GC-MS analysis of produced bio-oils. The column was an HP 235–



INNOWAX with 60 m length, 0,250 mm inner diameter, 0.25  $\mu\text{m}$  film having temperature limits between 40  $^{\circ}\text{C}$  to 300  $^{\circ}\text{C}$ . GC and the injector temperatures were the same during analysis. Helium was used as the carrier gas at a flow rate of 1.7 ml/min. 1  $\mu\text{L}$  samples was injected with a split ratio of 1:20. The GC oven temperature program was as follows: start at 40  $^{\circ}\text{C}$ ; hold for 10 min, raise from 40  $^{\circ}\text{C}$  to 200  $^{\circ}\text{C}$  at a heating rate of 5  $^{\circ}\text{C}/\text{min}$ ; hold for 15 min, raise to 240  $^{\circ}\text{C}$  at a heating rate of 10  $^{\circ}\text{C}/\text{min}$ ; hold for 15 min, raise to 260  $^{\circ}\text{C}$  at a heating rate of 10  $^{\circ}\text{C}/\text{min}$ ; hold at the final temperature for 10 min. The end of column was directly introduced into the ion source of a mass selective detector of Agilent 5975C series with operating conditions of transfer line at 270  $^{\circ}\text{C}$ , ion source at 250  $^{\circ}\text{C}$  and electron energy of 70 eV. Identification of bio-oil components was done using mass spectral libraries (PMW\_ToX3.1, Wiley7n.1 and NIST05a.L). During pyrolysis of *Thalassiosira weissflogi* and model compounds, the produced gases were collected in a gas bag and analyzed by a MKS Cirrus Mass Spectrometer.

### 2.3.5. Coke analysis

The amount of coke deposited on each catalyst was determined by the weight change during combustion using a thermogravimetric analyzer (TGA Q500). The burning of coke was carried out. 30 mg of sample in the alumina crucible were heated from 25 $^{\circ}\text{C}$  to the final temperature of 900 $^{\circ}\text{C}$  at a rate of 10 $^{\circ}\text{C}/\text{min}$  under a 70 mL/ min air atmosphere.

### 2.4. Pyrolysis experiments

The pyrolysis experiments of *Thalassiosira weissflogi* and its model compounds were performed using a fixed-bed reactor (Aysu and Sanna, 2015). The biomass sample was dried at 110 $^{\circ}\text{C}$  overnight before pyrolysis runs.  $\text{N}_2$  gas was fed at a flow rate of 15 ml/min for 10 min to remove the air in the reactor before pyrolysis. In a typical run, 3g dried *Thalassiosira weissflogi* powder or dried *Thalassiosira weissflogi*/catalyst (1:1) mixture or model compound/catalyst (1:1) mixture was placed in to the reactor in a ceramic container. Then, the

reactor was closed tightly and N<sub>2</sub> gas flow through. An external electric furnace was used to heat the reactor during which the temperature was controlled by a temperature controller. The algae pyrolysis experiments were performed at temperatures of 400, 500 and 600°C at a constant heating rate of 100 °C/min, with and without catalyst. The model compounds pyrolysis tests were carried out only without catalyst and in presence of CeO<sub>2</sub>. The reactor was kept constant at the final temperature for 60 min. The oil-condensation system was made of 3 Dreschel bottles maintained at 0°C using a ice-water bath. The gaseous products were not collected and vented out. The condensed bio-oils were recovered using acetone. The reactor was also washed with 100 ml of acetone to account for oil condensed between the heated region and the condensation set-up. Carryover of char into the condensation system was not noticed in any of the run, so that the bio-char recovered from the reactor represented the totality of it. Then the solvent was evaporated at 40°C and 11 kPa using a rotary evaporator to recover the oil which was recorded as bio-oil yield. When the reactor was cooled to room temperature, the remaining solid left behind was taken out, weighed and recorded as bio-char yield (subtracting the catalyst weight). The pyrolysis experiments without catalysts (400°C and 500°C) and in presence of CeO<sub>2</sub> (500°C) and Ce/Al<sub>2</sub>O<sub>3</sub> (500°C) were carried out in triplicate to evaluate the standart deviations (STD) (Table S1). STD on bio-char and bio-oil yields were between 0.17 and 1.96. Average values were reported. The total volatiles (liquid+gas yield) of *Thalassiosira weissflogi* in pyrolysis was calculated by subtraction of amount of solid (bio-char) left behind in the reactor. The amount of gaseous products was calculated by subtraction of solid and liquid yields from the amount of initial raw material (3 g). The following equations were used to calculate the total volatiles and product distribution (yields) of pyrolysis experiments:

$$\text{Total volatiles (\%)} = \frac{(W_{\text{Biomass,db}} - W_{\text{Solid,db}})}{W_{\text{biomass,db}}} \times 100 \quad (1)$$

$$\text{Liquid yield (wt \%)} = \frac{(W_{\text{Liquid}})}{W_{\text{Biomass,db}}} \times 100 \quad (2)$$

$$\text{Solid yield (wt \%)} = \frac{(W_{\text{Solid,db}})}{W_{\text{Biomass,db}}} \times 100 \quad (3)$$

$$\text{Gas yield (wt \%)} = 100\% - \text{liquid yield (wt \%)} - \text{solid yield (wt \%)} \quad (4)$$

where  $W_{\text{Biomass, db}}$  and  $W_{\text{Solid, db}}$  are the weights of initial algal biomass and remaining solid (bio-char) respectively on dry basis. The distribution of the parent algal material energy in the pyrolysis products was calculated considering the energy content of the different materials (microalgae, bio-oil, bio-char, bio-gas (by difference) and the pyrolysis material balance. Firstly, the product yields (%) of bio-char and bio-oil were determined by weighting the material collected into the condensation trap (bio-oil) and that left into the reactor (bio-char). Then, the gas yield was calculated by difference. The energy content of each product (bio-char and bio-oil) was calculated by multiplying the HHVs to the wt% of the products recovered. The energy content of bio-gas was calculated by subtracting the energy content of the bio-char and bio-oil from the starting energy content of the raw material (microalgae).

### 3. Results and discussion

#### 3.1. Raw material and catalysts characterization

*Thalassiosira weissflogi* (Table S.2) contains relatively high amount of proteins (43%) and low lipids (5%) and carbohydrates (12%). The *Thalassiosira weissflogi* low lipid content renders this alga not ideal for biodiesel production, but suitable for pyrolysis. The high protein content is in good agreement with literature and consistent with other algal species studied for production of biofuels such as *Nannochloropsis* and *Dunaliella* (Brown et al., 2010; Kim et al., 2015). Accordingly, the nitrogen content was high (4.64 wt%) due to high protein content. Ultimate analysis shows that *Thalassiosira weissflogi* has relatively high carbon content (38.84 wt%) on dry basis which makes it a suitable feedstock for biofuel production, while the proximate analysis shows high ash content (40 wt%). Thermogravimetric and DTG analysis of *Thalassiosira weissflogi* (Fig. 1) was performed to determine its thermal behaviour.

Overall, the pyrolysis curves can be divided into three stages: dehydration, devolatilization, and decomposition of the carbonaceous matter. There were seven main decomposition steps of which, the two at  $T < 130^\circ\text{C}$  corresponds to dehydration and short chain fatty acids decomposition. The four decomposition events between 200 and  $500^\circ\text{C}$  are related to algae compounds devolatilization and the final decomposition event at  $T > 650^\circ\text{C}$  corresponds to the decomposition of char formed in the previous steps. As indicated by TGA analysis, the decomposition stages between 200 and  $500^\circ\text{C}$  involved cellulose ( $375^\circ\text{C}$ ), proteins ( $220$  and  $300^\circ\text{C}$ ) and lipids ( $460^\circ\text{C}$ ) volatilisation. The latter event may also involve proteins decomposition. The high amount of solid residue left behind (51 %) after  $800^\circ\text{C}$  represents fixed carbon and inorganic materials (ash) in the parent material. The TGA shows that the initial decomposition temperature and the maximum weight loss rate of *Thalassiosira weissflogi* were lower than those of lignocellulosic biomass (Yuan et al., 2015; Maddi et al., 2011). For lignocellulosic biomass, the primary classes of thermally degradable biopolymers are hemicelluloses, cellulose and lignin. Hemicelluloses, cellulose and lignin decompose in the temperature range of  $220\text{--}315^\circ\text{C}$ ,  $315\text{--}400^\circ\text{C}$  and from 200 to  $900^\circ\text{C}$ , respectively (Yang et al., 2007). The main reason for the shifting at lower temperature of the microalgae devolatilisation is attributed to the absence of lignin, which results in a complete volatilisation of *Thalassiosira weissflogi* at  $500^\circ\text{C}$ . Extractives, triglycerides and hexane soluble components in microalgae are less thermal resistant than lignin present in lignocellulosic biomass (Sanchez-Silva et al., 2012).

The total pore volume, specific surface area (BET) and average pore diameter of  $\text{Al}_2\text{O}_3$  support were  $0.129\text{ cm}^3/\text{g}$ ,  $75.39\text{ m}^2/\text{g}$ , and  $37.44\text{ \AA}$ , respectively. Addition of metal oxide to  $\text{Al}_2\text{O}_3$  influenced the catalyst properties. Surface area and pore volume were decreased, while pore size was increased slightly. Surface areas of  $\text{Ce}/\text{Al}_2\text{O}_3$ ,  $\text{NiCe}/\text{Al}_2\text{O}_3$ , and  $\text{MgCe}/\text{Al}_2\text{O}_3$  were found to be 55.1, 60.2, and  $49.6\text{ m}^2/\text{g}$ , respectively (Aysu and Sanna, 2015). The X-ray

diffraction patterns of the prepared catalysts with  $\text{Al}_2\text{O}_3$  support are shown in the Supplementary data (Fig. S1-a,b,c). XRD diffraction patterns confirm the formation of the metal oxides ( $\text{CeO}_2$ ,  $\text{NiO}$ ,  $\text{MgO}$ ) with exact matches. XRD patterns of  $\text{Ce}/\text{Al}_2\text{O}_3$  catalyst (Fig. S1-a,b,c) exhibit peaks ( $2\theta$  scale) at  $28.5^\circ$ ,  $33.10^\circ$ ,  $47.60^\circ$ ,  $56.39^\circ$ ,  $59.13^\circ$ ,  $69.51^\circ$  and  $79.10^\circ$  attributed to the cubic cerium (IV) oxide crystal phase. XRD patterns of  $\text{Ni-Ce}/\text{Al}_2\text{O}_3$  (Fig. S1-b) show peaks that match the cubic nickel (II) oxide at  $2\theta$  scale =  $37.20^\circ$ ,  $43.18^\circ$ ,  $62.90^\circ$ ,  $75.22^\circ$ , and  $79.40^\circ$ .  $\text{Mg-Ce}/\text{Al}_2\text{O}_3$  (Fig. S1-c) catalyst shows peaks for cubic magnesium oxide ( $\text{MgO}$ ) crystal at  $2\theta$  scale= $37.00^\circ$ ,  $43.00^\circ$ ,  $62.30^\circ$ , and  $78.50^\circ$ . These results were consistent with those previously reported in literature (Qiao et al., 2009; Hernández-Enríquez et al., 2012; Aysu and Sanna, 2015).

### 3.2. Effect of temperature on product distribution

The total volatiles and distribution of products obtained by pyrolysis of *Thalassiosira weissflogi* at different temperatures with (1:1 ratio) and without catalyst are given in Table

S.3. High char yields are probably due to the slow heating rate used ( $100^\circ\text{C}/\text{min}$ ) during pyrolysis (Kersten et al., 2005). The total volatiles and the gas yields were increased generally, while the bio-char yields decreased in all experiments. The highest liquid yield of 25.8% was achieved with  $\text{CeO}_2$  at  $500^\circ\text{C}$ . The effect of temperature on changing the products yields was limited, probably due to the use of a batch reactor operating with slow heating rates. Ni-Ce on alumina support had a positive effect on cracking and minimising char at  $400$  and  $500^\circ\text{C}$ , while mainly boosted gas formation at  $600^\circ\text{C}$ , compared to the other tested catalysts. Therefore, NiCe-Alumina actively promoted secondary cracking reactions of char (Rover et al., 2014; Li et al., 2012). This trend is in agreement with our previous study on *Nannochloropsis* catalytic pyrolysis, where  $\text{Ni-Ce}/\text{Al}_2\text{O}_3$  resulted in good deoxygenation effect at  $500^\circ\text{C}$  (Aysu and Sanna, 2015).

### 3.3. Effect of catalysts on product distribution

The catalysts used in this study exhibited a negligible effect on product yields (Table S.3).

However, the use of ceria catalysts affected the quality of the products from the microalgae and model compounds as discussed in the following sections. The highest total volatiles (85.8%) were obtained with NiCe/Al<sub>2</sub>O<sub>3</sub> at 600°C. This can be related to the secondary cracking of tars in presence of Ni on alumina support and to the larger surface areas and pore volumes of NiCe/Al<sub>2</sub>O<sub>3</sub> compared to the other doped catalysts (Díaz-Rey et al., 2014). CeO<sub>2</sub> based catalysts catalyse ketonisation and aldol condensation of carbonyl compounds in pyrolysis vapour with rejection of the oxygen of carboxylic acid as CO<sub>2</sub> and water, due to their facile reduction/oxidation and acid–base properties (Alonso et al., 2010).

In terms of energy recovery, most of the starting microalgae energy was recovered in the bio-oils as can be seen in Fig. 2. CeO<sub>2</sub> and NiCe/Al<sub>2</sub>O<sub>3</sub> were the most effective catalysts, which maintained 82.8% (daf) and 76.0% (daf) of the starting energy in the bio-oils respectively. This indicates that deoxygenation of *Thalassiosira weissflogi* in presence of CeO<sub>2</sub> and Ce/Ni-alumina is very effective compared to deoxygenation of other microalgae under the same conditions (Aysu and Sanna, 2015).

Fig. 3 shows the nitrogen distribution in the products of catalytic and non-catalytic pyrolysis of *Thalassiosira weissflogi* at 500°C. Bio-oil obtained without catalyst contained about 41.5 wt% of the nitrogen, while 11.5 wt% remained in the solid bio-char and 47.0 wt% went into the gas products. From a fuel quality point of view, nitrogen in bio-oil is detrimental. The use of Ce-catalysts lowered the nitrogen content in the bio-oils. MgCe/Al<sub>2</sub>O<sub>3</sub> was most effective catalyst in removing nitrogen from bio-oil (19.4%) and released the most of nitrogen (69.7%) as uncondensable gases, while keeping only 10.9% in bio-char. Also, Ce/Al<sub>2</sub>O<sub>3</sub> (24.2%) and NiCe/Al<sub>2</sub>O<sub>3</sub> (27.8%) were able to consistently reduce the N content in bio-oils, compared to without catalyst. These N removal data are comparable with those obtained by pre-treating microalgae (e.g. *Nannochloropsis*) with low temperature hydrothermal liquefaction (225°C,

15 min) and then subjecting the solid residue to hydro-thermal liquefaction (350°C, 60 min) (Costanzo et al., 2015). Moreover, previous work showed that nitrogen sent to gas phase can be recycled in a loop process to feed microalgae and boost their growth (Wang et al., 2013; Jena, 2011).

TGA of the spent (coked) catalysts was carried out in pure air to evaluate the amount of coke formed on catalysts. Figs. S.2-S.5 show the TGA curves of the coked catalysts. Initial mass loss between 25 and 100 °C was associated to release of absorbed water. The second mass loss between 100 and 600°C was associated to decomposition of the char, while the third (final) mass loss between 600 and 900 °C was associated to coke combustion. NiCe/Al<sub>2</sub>O<sub>3</sub> had the lowest amount of coke (5.2%) while MgCe/Al<sub>2</sub>O<sub>3</sub> had the highest (7.5%). This is in agreement with the pyrolysis mass balance (Table S.3), which shows their catalytic activities in terms of high total volatiles. Oxygen affinity of Ce improved the activity of Ni/Al<sub>2</sub>O<sub>3</sub> catalyst in terms of coke suppression. Adsorbed O species in presence of Ce and Ni, due to lattice O and redox properties of Ce forms gas species such as CO<sub>2</sub> and CO instead of coke deposition (Oemar et al., 2014). Fig. 4-d also suggests that CeO<sub>2</sub> oxygen affinity can promote oxidation of coke with formation of CO.

#### 3.4. Characterization of bio-chars and bio-oils by EA, TGA, <sup>1</sup>H NMR and GC–MS analysis.

The elemental analysis of bio-chars obtained from *Thalassiosira weissflogi* pyrolysis (Table S.4) showed their lower calorific values (5-9 MJ/kg) compared to that of raw material (11 MJ/kg). This is because most of the starting microalgae energy was maintained in the bio-oils.

Due to their low energy content, bio-chars may be utilized as soil amendment as they contain high ash and nitrogen (~3%) contents. The EA (daf) of the bio-char indicates that the C content is lower than typical bio-chars and richer in O. High O content can be related to low-temperature pyrolysis, which produces biochar enriched in volatile-matter composition with relatively high O content. Low C content is attributed to the high ash content (~ 80%) in the

Thalassiosira W. derived bio-chars. Typically, microalgae ash is rich in Si, which can favour the formation of the Si–C bonds, thereby increasing the number of aromatic components and recalcitrance of the bio-chars as a result of temperatures (Jindo et al, 2014). A previous study reported that the presence of silicon in rice husk biochar obtained at 500 °C formed a dense carbon structure with Si-encapsulated carbon; in contrast, in the bio-chars prepared at the temperature of 700 °C, the silicon component was physically distanced from the carbon structure (Guo and Chen, 2014).

The HHVs and elemental analysis of bio-oils from *Thalassiosira weissflogi* are given in Table 1. All catalysts increased C and H content in bio-oils and consequently enhanced their energy content. The most effective catalysts in improving bio-oil energy content were CeO<sub>2</sub> and MgCe/Al<sub>2</sub>O<sub>3</sub> which increased the HHVs of bio-oils up to 35.37 and 36.37 MJ/kg, respectively, compared to non-catalytic run (32.85 MJ/kg). High nitrogen contents of bio-oils, which comes from chlorophyll and proteins in *Thalassiosira weissflogi* was somehow reduced in both bio-char and bio-oil and preferentially send to gas phase when the catalysts were used. Bio-oil from *Thalassiosira weissflogi* had lower oxygen content than bio-oils from pyrolysis of lignocellulosic biomass, which makes it more suitable for fuel use. CeO<sub>2</sub> was the most effective catalyst in reducing O<sub>2</sub> content (12.28%) in bio-oil compared to in absence of catalysts (15.81%). When considering the elemental analysis of bio-oils obtained from pyrolysis of the microalgae model compounds with CeO<sub>2</sub> (Table 2), it can be noticed that CeO<sub>2</sub> increased the C content of fatty acids bio-oil and H content for all the model compounds, while it decreased N content in protein derived bio-oil and O content in fatty acids and cellulose bio-oils. In contrast, the O content was slightly increased in bio-oil derived from protein pyrolysis.

The proximate analysis of *Thalassiosira weissflogi* and model compounds bio-oils were determined by TGA (Tables S.5 and S.6). Most of the bio-oils mainly contain volatiles with



negligible amount of fixed carbon (except cellulose bio-oils) and ash, which is important in terms of bio-fuels production.

The integration of the  $^1\text{H}$ NMR spectra of the *Thalassiosira weissflogi* and model compounds bio-oils obtained without and with catalysts are presented in Tables 3 and 4, respectively. As seen in Table 3, there were clear differences in the overall chemical composition of the *Thalassiosira weissflogi* bio-oils from different catalysts. The region (0 to 1.6 ppm) representing aliphatic proton was the most populated for the bio-oils indicating their higher aliphatic content. Almost all catalysts have increased the aliphatics products and decreased the total oxygenates compared to non-catalytic run. Bio-oils obtained in the presence of  $\text{CeO}_2$  and  $\text{NiCe}/\text{Al}_2\text{O}_3$  contained the highest percentage of aliphatic protons (~59 and ~62 % of all). The regions (1.6 to 2.2 ppm and 2.2 to 3.0 ppm) which represent proton on aliphatic carbon atoms bonded to a C=C double bond (olefinic or aromatic) or two bonds away from a heteroatom (O or N) were abundant in the bio-oil obtained with  $\text{CeO}_2$  and  $\text{MgCe}/\text{Al}_2\text{O}_3$ . The protons in the region (4.2-6.4 ppm) that represents aromatic ether (such as methoxyphenols) and carbohydrate-like molecules were in small amounts (~1-6%) in all bio-oils. This is consistent with the low O content in bio-oils from EA (Table 1). The distribution of the protons in the aromatics and N/O heteroaromatics regions (6.4-6.8 and 6.8-8 ppm) indicate that  $\text{CeO}_2$  did not affect aromatics production compared to the run in absence of catalyst, while  $\text{NiCe}/\text{Al}_2\text{O}_3$  increased the aromatics. Aldehydes and carboxylic acids (8-10 ppm) were not detected in all bio-oils. When we look at the  $^1\text{H}$  NMR results of model compounds (Table 4), we see that  $\text{CeO}_2$  reduced the total oxygenates and increased aliphatics products in cellulose and protein pyrolysis. Proteins also produced aromatics. Instead, Ce-catalysts did not affect fatty acids pyrolysis, where both non-catalytic and catalytic bio-oils were rich in aliphatics.

GC-MS analysis of the *Thalassiosira weissflogi* and its model compounds bio-oils produced at 500°C was carried out in order to determine the main products. While NMR is able to give a picture of the whole bio-oil composition, the GC-MS technique is limited to the identification of the components with boiling point up to 270°C, which corresponds to the highest temperature used in the GC-MS analysis. The list of the main functionalities identified by GC-MS- from pyrolysis of *Thalassiosira weissflogi* is given in Table 5 (Identified compounds are listed in Table S.7). Represented chemical functionalities are consistent with those detected by <sup>1</sup>H NMR. While major compounds were found in all bio-oils, catalysts affected both their number and distribution. Owing to complex nature of pyrolysis bio-oils and bio-oil TGAs, about 80% of the bio-oils compounds were identified by GC-MS, which consistently confirmed the EA, TGA and NMR data. Bio-oils produced from pyrolysis of *Thalassiosira weissflogi* are complex mixture of organic compounds with different molecular structures and molecular weights. These compounds can be divided into several functional groups: aliphatics, monoaromatics, oxygenated compounds, nitrogen containing compounds and their derivatives. As confirmed by proton NMR, majority of the compounds were aliphatics (alkanes and alkenes), which were mainly generated from the conversion of saturated and unsaturated fatty acids in algal cells and protein branches. Bio-oils contained relatively high levels of long-chain alkanes which contribute to the good combustion property. The nitrogen containing compounds in bio-oils, such as indole, nitriles, amines, and amides derived from protein degradation in algal cells. Large amount of ketones were formed from partial decarboxylation and decarbonylation reactions. The main aromatics were phenol, phenol substitutes and benzenes. Phenolics were formed in relatively low amount than other compounds as algae contain no lignin in their structure. The carbon and hydrogen contents of obtained bio-oils were close to conventional fossil fuels but the content of oxygen and nitrogen were still high. Combustion of nitrogen in fuels forms undesirable NO<sub>x</sub> compounds.

### 3.5. Pyrolysis mechanism

The  $^1\text{H}$  NMR analysis (Tables 3 and 4) of *Thalassiosira weissflogi* and model compounds indicate that ceria increased the aliphatics products and decreased oxygenates through deoxygenation. This trend was supported by EA (Table 2), where carbon and hydrogen content increased and oxygen decreased more in presence of ceria. Also, the elemental analysis and mass balance calculations show that nitrogen decreased in *Thalassiosira weissflogi* and protein bio-oils indicating nitrogen removal in presence of ceria.

To establish the deoxygenation pathways and to find the production pathways of the major compounds in algal bio-oils, gas analysis (MS) of *Thalassiosira weissflogi* and its model compounds (cellulose, egg white powder and palm-jojoba oils mixture) was performed. The GC-MS analysis of the oils was also carried out and correlated to the gas analysis (MS) and  $^1\text{H}$  NMR analysis to study the pyrolysis reaction mechanism.

Gas (MS) analysis (Fig. 4, a-d) clearly indicates that dehydration and decarboxylation were the main reactions involved in the algae and model compounds deoxygenation in absence of catalyst, while  $\text{CeO}_2$  also promoted decarbonylation (Fig. 4-d). Nitrogen was removed as ammonia gas ( $\text{NH}_3$ ) and hydrogen cyanide (HCN). Oxygen from cellulose was eliminated as  $\text{CO}_2$  and  $\text{H}_2\text{O}$ . Ceria ( $\text{CeO}_2$ ) increased the dehydration and decarbonylation compared to in absence of catalyst (Fig. 4-a).  $\text{CeO}_2$  based catalysts have been investigated for their capacity to catalyse ketonisation and aldol condensation of carbonyl compounds in pyrolysis vapour with the oxygen of carboxylic acid is rejected as  $\text{CO}_2$  and water.  $\text{CeO}_2$  is highly active for this purpose and tolerant to water. The catalytic activity of ceria based materials is due to their facile reduction/oxidation and acid-base properties (Alonso et al., 2010).

GC-MS analysis of cellulose bio-oils (Table 6 and Table S.7) shows levoglucosan (90.4%) as main product, while cellulose was partially re-arranged to smaller compounds in presence of  $\text{CeO}_2$  such as isopropyl acetate, 2 (3H)-furanone, 2-hydroxy-gamma-butyrolactone and

cyclopentanone. The GC analysis of bio-oil from fatty acids (Fig. 4-b) clearly shows that decarboxylation reactions were enhanced by CeO<sub>2</sub>. This is supported by GC-MS results (Table 6 and Table S.8), where less amount of carboxylic acids (from fatty acids) such as palmitic, linoleic and capric acid were detected in presence of ceria. Decarboxylation led to paraffinic compounds, both linear and cyclic and favoured the production of ketones (2-Heptadecanone, 3-Tetradecanone, 2-Nonadecanone). Ceria promoted the decarbonylation and decarboxylation of model protein (egg white powder) and *Thalassiosira weissflogi* during pyrolysis (Fig. 4-c, 4-d). Removal of nitrogen compounds from proteins was favoured in presence of CeO<sub>2</sub> as NH<sub>3</sub> and HCN. Pyrolysis of proteins (Table 6 and Table S.8) produced aromatic compounds such as indole, pyrroles, skatole, phenyl ethanol and phenol. CeO<sub>2</sub> also showed high selectivity towards ketones. Large amount of ketones were formed from the partial decarboxylation and decarbonylation of *Thalassiosira* microalga (57% by GC-MS) and its fatty acids and proteins compounds. CeO<sub>2</sub> showed better cracking because of acid sites and reduced the total amount of aldehydes, which are undesirable due to their poor thermal stability.

#### 4. Conclusion

The catalytic pyrolysis of *Thalassiosira weissflogi* and its three major components in presence of ceria catalysts was studied. Light oxygenates, aromatics and aliphatics were originated from carbohydrates, proteins and lipids components, respectively. Dehydration and decarboxylation were the main reactions involved in deoxygenation, while nitrogen was removed as NH<sub>3</sub> and HCN. CeO<sub>2</sub> increased decarbonylation reactions compared to in absence of catalyst, with production of ketones. Ceria catalysts were able to consistently reduce the N-content in bio-oil to 20-38% of that in the parent material and reduce the formation of coke due to its excellent redox properties and coke oxidation by decarbonylation.

#### Acknowledgements

The authors thank the Centre for Innovation in Carbon Capture and Storage (CICCS), Heriot-Watt University (EPSRC Grant No. EP/F012098/2) for support and Varicon Aqua Solutions for providing the algae sample. Tefvik Aysu thanks the financial support provided by the post-doctoral research fellowship programme (2219), Scientific and Technological Research Council of Turkey (TUBITAK).

## References

1. Abdullah, N., Gerhauser, H., 2008. Bio-oil derived from empty fruit bunches. *Fuel* 87, 2606–2613.
2. Alonso, D.M., Bond, J.Q., Dumesic, J.A., 2010. Catalytic conversion of biomass to biofuels. *Green Chem.* 12, 1493–1513.
3. Aysu, T., 2015. Catalytic pyrolysis of *Alcea pallida* stems in a fixed-bed reactor for production of liquid bio-fuels. *Bioresource Technol.* 191, 253-262.
4. Aysu, T., Sanna, A., 2015. Nannochloropsis algae pyrolysis with ceria-based catalysts for production of high-quality bio-oils. *Bioresource Technol.* 194, 108-116.
5. Brown, T.M., Duan, P., Savage, P.E., 2010. Hydrothermal liquefaction and gasification of *Nannochloropsis* sp. *Energy Fuels* 24, 3639-3646.
6. Costanzo, W., Jena, U., Hilten, R., Das, K.C., Kastner, J.R., 2015. Low temperature hydrothermal pretreatment of algae to reduce nitrogen heteroatoms and generate nutrient recycle streams, *Algal Research* 12, 377–387.
7. Díaz-Rey, M.R., Cortés-Reye, M., Herrera, C., Larrubia, M.A., Amadeo, N., Laborde M, Alemany L.J., 2014. Hydrogen-rich gas production from algae-biomass by low temperature catalytic gasification. *Catal. Today* 257, 2, 177–184.
8. Du, Z., Hu, B., Ma, X., Cheng, Y., Liu, Y., Lin, X., Wan, Y., Lei, H., Chen, P., Ruan, R., 2013. Catalytic pyrolysis of microalgae and their three major components: Carbohydrates, proteins, and lipids. *Bioresource Technol.* 130, 777–782.

9. Fisk, C.A., Morgan, T., Ji, Y., Crocker, M., Crofcheck, C., Lewis, S.A., 2009. Bio-oil upgrading over platinum catalysts using in situ generated hydrogen. *Appl. Catal. A-Gen.* 358, 150–156.
10. Gai, C., Zhang, Y., Chen, W.T., Zhang, P., Dong, Y., 2015. An investigation of reaction pathways of hydrothermal liquefaction using *Chlorella pyrenoidosa* and *Spirulina platensis*. *Energy Convers. Manage.* 96, 330–339.
11. Gerpen, J.V., 2005. Biodiesel processing and production. *Fuel Process. Technol.* 86, 1097-1107.
12. Gopakumar, S.T., Adhikari, S., Chattanathan, S.A., Gupta, R.B., 2012. Catalytic pyrolysis of green algae for hydrocarbon production using H+ZSM-5 catalyst. *Bioresource Technol.* 118, 150–157.
13. Guo, J. and Chen, B., 2014. Insights on the molecular mechanism for the recalcitrance of biochar: interactive effects of carbon and silicon components. *Environ. Sci. Technol.* 48, 9103–9101.
14. Hernández-Enríquez, J.M., Silva-Rodrigo, R., García-Alamilla, R., García-Serrano, L.A., Handy, B.E., Cárdenas-Galindo, G., Cueto-Hernández, A., 2012. Synthesis and Physico-Chemical Characterization of  $\text{CeO}_2/\text{ZrO}_2\text{-SO}_4^{2-}$  Mixed Oxides. *J. Mexican Chem. Soc.* 56, 115-120.
15. Jena, U., Thermochemical conversion of microalgal biomass for production of biofuels and co-products. PhD Thesis. Athens, Georgia, 2011.
16. Jindo K., Mizumoto H., Sawada Y., Sanchez-Monedero M.A., Sonoki T., 2014. Physical and chemical characterization of biochars derived from different agricultural residues, *Biogeosciences*, 11, 6613–6621.

17. Kersten, S.R.A., Wang, X., Prins, W., van Swaij, W.P.M., 2005. Biomass pyrolysis in a fluidized bed reactor. Part I: Literature review and model simulations. *Ind. Eng. Chem. Res.* 44, 8773–8785.
18. Kim, S.S., Ly, H.V., Kim, J., Lee, E.Y., Woo, H.C., 2015. Pyrolysis of microalgae residual biomass derived from *Dunaliella tertiolecta* after lipid extraction and carbohydrate saccharification. *Chem. Eng. J.* 263, 194–199.
19. Li, R., Zhong, Z.P., Jin, B.S., Zheng, A.J., 2012. Selection of temperature for bio-oil production from pyrolysis of algae from lake blooms. *Energy Fuels* 26, 2996–3002.
20. Maddi, B., Viamajala, S., Varanasi, S., 2011. Comparative study of pyrolysis of algal biomass from natural lake blooms with lignocellulosic biomass. *Bioresource Technol.* 102, 11018–11026.
21. Maguyon, M.C.C., Capareda, S.C., 2013. Evaluating the effects of temperature on pressurized pyrolysis of *Nannochloropsis oculata* based on products yields and characteristics. *Energy Convers. Manage.* 76, 764–773.
22. Na, J.G., Han, J.K., Oh, Y.K., Park, J.H., Jung, T.S., Han, S.S., Yoon, H.C., Chung, S.H., Kim, J.N., Ko, C.H., 2012. Decarboxylation of microalgal oil without hydrogen into hydrocarbon for the production of transportation fuel. *Catal. Today* 185, 313–317.
23. Oemar, U., Li, A.M., Hidajat, K., Kawi, S., 2014. Mechanism and kinetic modeling for steam reforming of toluene on  $\text{La}_{0.8}\text{Sr}_{0.2}\text{Ni}_{0.8}\text{Fe}_{0.2}\text{O}_3$  catalyst, *AIChE Journal* 60, 4190–4198.
24. Peng, W., Wu, Q., Tu, P., Zhao, N., 2001. Pyrolytic characteristics of microalgae as renewable energy source determined by thermogravimetric analysis. *Bioresource Technol.* 80, 1–7.

25. Rover, M.R., Johnston, P.A., Whitmer, L.E., Smith, R.G., Brown, R.C., 2014. The effect of pyrolysis temperature on recovery of bio-oil as distinctive stage fractions, *J. Anal. Appl. Pyrol.* 105, 262–268.
26. Qiao, H., Wei, Z., Yang, H., Zhu, L., Yan, X., 2009. Preparation and Characterization of NiO Nanoparticles by Anodic Arc Plasma Method. *J. Nanomaterials* 64, 1-5.
27. Sanchez-Silva, L., López-González, D., Villasenor, J., Sanchez, P., Valverde, J., 2012. Thermogravimetric-mass spectrometric analysis of lignocellulosic and marine biomass pyrolysis. *Bioresource Technol.* 109, 163–172.
28. Trinh, T.N., Jensen, P.A., Dam-Johansen, K., Knudsen, N.O., Sørensen, H.R., Hvilsted, S., 2013. Comparison of lignin, macroalgae, wood, and straw fast pyrolysis. *Energy Fuels* 27, 1399–1409.
29. Vardon, D.R., Sharma, B.K., Blazina, G.V., Rajagopalan, K., Strathmann, T.J., 2012. Thermochemical conversion of raw and defatted algal biomass via hydrothermal liquefaction and slow pyrolysis. *Bioresource Technol.* 109, 178–187.
30. Wang, K., Brown, R.C., Homsy, S., Martinez, L., Sidhu, S.S., 2013. Fast pyrolysis of microalgae remnants in a fluidized bed reactor for bio-oil and biochar production. *Bioresource Technol.* 127, 494–499.
31. Wang, K., Brown, R.C., 2013. Catalytic pyrolysis of microalgae for production of aromatics and ammonia. *Green Chem.* 15, 675-681.
32. Wang, K., Kima, K.H., Brown, R.C., 2014. Catalytic pyrolysis of individual components of lignocellulosic biomass. *Green Chem.* 16, 727-735.
33. Yang, H., Yan, R., Chen, H., Lee, D.H., Zheng, C., Characteristics of hemicellulose, cellulose and lignin pyrolysis. *Fuel* 2007; 86, 1781–8.



34. Ying, X., Tiejun, W., Longlong, M., Guanyi, C., 2012. Upgrading of fast pyrolysis liquid fuel from biomass over Ru/ $\gamma$ -Al<sub>2</sub>O<sub>3</sub> catalyst. *Energy Convers. Manage.* 55, 172–177.
35. Yuan, T., Tahmasebi, A., Yu, J., 2015. Comparative study on pyrolysis of lignocellulosic and algal biomass using a thermogravimetric and a fixed-bed reactor. *Bioresource Technol.* 175, 333–341.

### Figures Captions

**Figure 1.** Thermogravimetric profile of *Thalassiosira weissflogi* and its derivative analysis.

**Figure 2.** Energy (daf) distribution in the pyrolysis products.

**Figure 3.** Nitrogen (N) distribution in the pyrolysis products.

**Figure 4.** Gas analysis in absence and presence of CeO<sub>2</sub> from the pyrolysis of (a) cellulose, (b) fatty acids, (c) proteins and (d) *Thalassiosira weissflogi*.

**Table 1** The results of elemental analysis of the *Thalassiosira weissflogi* bio-oils obtained at 500 °C.

Elemental analysis <sup>a</sup>	No catalyst	CeO <sub>2</sub>	Ce/Al <sub>2</sub> O <sub>3</sub>	NiCe/Al <sub>2</sub> O <sub>3</sub>	MgCe/Al <sub>2</sub> O <sub>3</sub>
Carbon	67.59	71.46	71.07	70.25	71.47
Hydrogen	8.90	9.30	9.34	9.42	10.21
Nitrogen	7.70	6.96	5.20	5.35	4.24
Oxygen <sup>b</sup>	15.81	12.28	14.39	14.98	14.08
H/C molar ratio	1.58	1.56	1.57	1.60	1.71
O/C molar ratio	0.17	0.12	0.15	0.16	0.14
HHV (MJ/kg)	32.85	35.37	34.92	34.65	36.37

<sup>a</sup> Weight percentage on dry and ash free basis. <sup>b</sup> By difference

**Table 2** Elemental analysis, H/C and O/C molar ratios and HHV of model compounds bio-oils obtained at 500 °C.

Elemental analysis <sup>a</sup>	Cellulose	Cellulose + CeO <sub>2</sub>	Egg white powder	Egg white powder+ CeO <sub>2</sub>	Palm-jojoba	Palm-jojoba+ CeO <sub>2</sub>
Carbon	46.13	46.52	58.20	57.99	74.70	78.52
Hydrogen	5.80	6.39	7.82	7.91	12.28	12.87
Nitrogen	-	-	11.97	10.97	-	-
Oxygen <sup>b</sup>	48.07	47.09	22.01	23.13	13.02	8.61
H/C molar ratio	1.50	1.64	1.61	1.63	1.97	1.96
O/C molar ratio	0.78	0.75	0.28	0.30	0.13	0.08
HHV (MJ/kg)	15.30	16.46	27.00	26.86	40.64	43.58

<sup>a</sup> Weight percentage on dry and ash free basis. <sup>b</sup> By difference

**Table 3**  $^1\text{H}$  NMR Integrations of *Thalassiosira weissflogii* bio-oils formed at 500 °C versus specific chemical shift ranges. nd: not detected.

Chemical shift region (ppm)	Type of protons	No catalyst	Hydrogen content (% of all hydrogen)			
			CeO <sub>2</sub>	Ce/Al <sub>2</sub> O <sub>3</sub>	NiCe/Al <sub>2</sub> O <sub>3</sub>	MgCe/Al <sub>2</sub> O <sub>3</sub>
0.0 – 1.6	-CH <sub>3</sub> , -CH <sub>2</sub> -	44.77	59.22	54.91	65.44	56.78
1.6 – 2.2	-CH <sub>2</sub> -, aliphatic OH	17.05	15.20	14.04	8.35	14.68
2.2 – 3.0	CH <sub>3</sub> OC-, CH <sub>3</sub> -Ar, -CH <sub>2</sub> Ar	19.38	11.47	10.99	4.86	11.85
3.0 – 4.2	CH <sub>3</sub> O-, -CH <sub>2</sub> O-, =CHO	8.17	4.88	7.81	4.01	4.90
4.2 – 6.4	=CHO, ArOH, HC=C	3.10	1.38	3.99	5.74	6.15
6.4 – 6.8	HC=C (nonconjugated)	0.29	0.73	1.03	1.72	0.68
6.8 – 8.0	ArH, HC=C (conjugated)	7.30	7.28	7.20	9.89	4.95
8.0 – 10.0	-CHO, -COOH, downfield	nd	nd	nd	nd	nd

**Table 4**  $^1\text{H}$  NMR Integrations of *Thalassiosira weissflogii* and model compounds bio-oils formed at 500 °C versus specific chemical shift ranges.

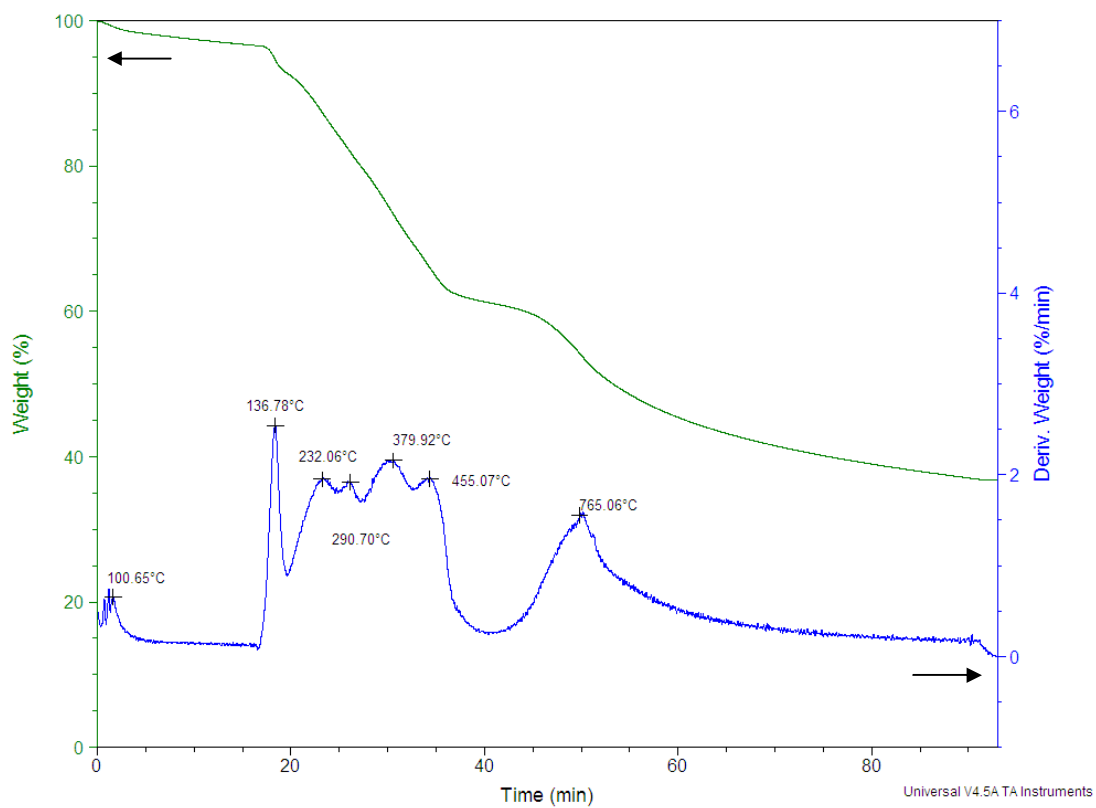
Chemical shift region (ppm)	Type of protons	Hydrogen content (% of all hydrogen)							
		No catalyst	CeO <sub>2</sub>	Cellulose	Cellulose + CeO <sub>2</sub>	Egg white powder	Egg white powder + CeO <sub>2</sub>	Palm-jojoba	Palm-jojoba + CeO <sub>2</sub>
0.0 – 1.6	-CH <sub>3</sub> , -CH <sub>2</sub> -	44.77	59.22	5.25	9.19	40.44	46.06	81.78	80.97
1.6 – 2.2	-CH <sub>2</sub> -, aliphatic OH	17.05	15.20	6.13	9.31	14.17	12.84	8.86	8.68
2.2 – 3.0	CH <sub>3</sub> OC-, CH <sub>3</sub> -Ar, -CH <sub>2</sub> Ar	19.38	11.47	7.03	8.24	17.89	19.90	4.38	4.55
3.0 – 4.2	CH <sub>3</sub> O-, -CH <sub>2</sub> O-, =CHO	8.17	4.88	43.8	43.73	11.59	8.86	0.35	0.90
4.2 – 6.4	=CHO, ArOH, HC=C	3.10	1.38	32.5	25.03	6.45	3.07	4.18	4.48
6.4 – 6.8	HC=C (nonconjugated)	0.29	0.73	1.04	0.93	1.46	0.85	0.02	0.02
6.8 – 8.0	ArH, HC=C (conjugated)	7.30	7.28	2.65	2.22	7.99	8.43	0.47	0.40
8.0 –	-CHO, -COOH, downfield	0.00	0.00	1.50	1.35	0.00	0.00	0.00	0.00

**Table 5** GC–MS analysis of bio-oil products of *Thalassiosira weissflogii* pyrolysis.

Compounds	Relative abundance (% area)				
	<i>No</i>	<i>CeO<sub>2</sub></i>	<i>Ce/Al<sub>2</sub>O<sub>3</sub></i>	<i>Ni-Ce/Al<sub>2</sub>O<sub>3</sub></i>	<i>Mg-Ce/Al<sub>2</sub>O<sub>3</sub></i>
	<i>catalyst</i>				
<b><i>Monoaromatics</i></b>	5.16	6.38	5.41	7.72	1.05
<b><i>Aliphatics</i></b>	27.76	12.10	28.52	49.20	69.70
<b><i>Alcohols</i></b>	16.10	4.22	6.53	0	1.1
<b><i>Aldehydes</i></b>	7.52	0.22	0	0	0
<b><i>Ketones</i></b>	14.57	57.36	18.81	20.26	18.82
<b><i>Carboxylic acids</i></b>	0	0	2.86	0	0.88
<b><i>Esters</i></b>	0	1.25	0	0	0.69
<b><i>Ethers</i></b>	0.54	5.94	11.79	0	0
<b><i>Nitrogen</i></b>	12.99	8.11	20.91	15.04	7.68
	<i>compounds</i>				
<b><i>Total</i></b>	84.64	95.58	94.83	92.22	99.92

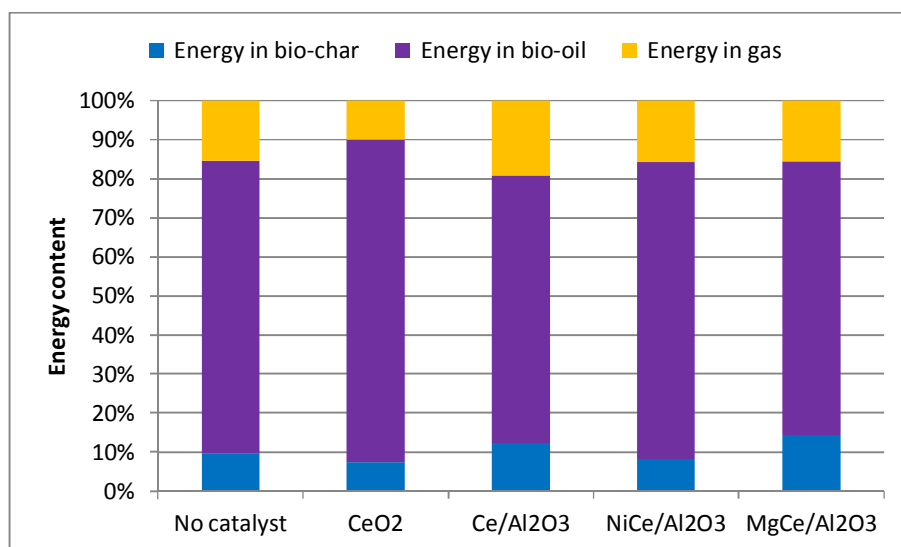
**Table 6** GC–MS analysis of bio-oil products of *Thalassiosira weissflogii* and model compounds pyrolysis.

Compounds	Relative abundance (% area)							
	No catalyst	CeO <sub>2</sub>	Cellulose	Cellulose+CeO <sub>2</sub>	Palm-jojoba	Palm-jojoba+CeO <sub>2</sub>	Egg white powder	Egg white powder + CeO <sub>2</sub>
<i>Monoaromatics</i>	5.16	6.38	0	0	0	0	12.40	8.34
<i>Aliphatics</i>	27.76	12.10	0	0.55	28.56	36.87	0	5.89
<i>Sugars</i>	0	0	94.67	88.61	0	0	0	0
<i>Alcohols</i>	16.10	4.22	0	2.14	0	0	10.97	8.36
<i>Aldehydes</i>	7.52	0.22	0.30	0.25	0	0	0	0
<i>Ketones</i>	14.57	57.36	5.03	5.92	0.70	13.05	2.35	7.41
<i>Carboxylic acids</i>	0	0	0	0	70.67	49.44	0	0
<i>Esters</i>	0	1.25	0	2.53	0	0.52	2.64	0
<i>Ethers</i>	0.54	5.94	0	0	0	0	0	0
<i>Nitrogen</i>	12.99	8.11	0	0	0	0	44.33	35.34
<i>Total</i>	84.64	95.58	100	100	99.93	99.88	72.69	65.34

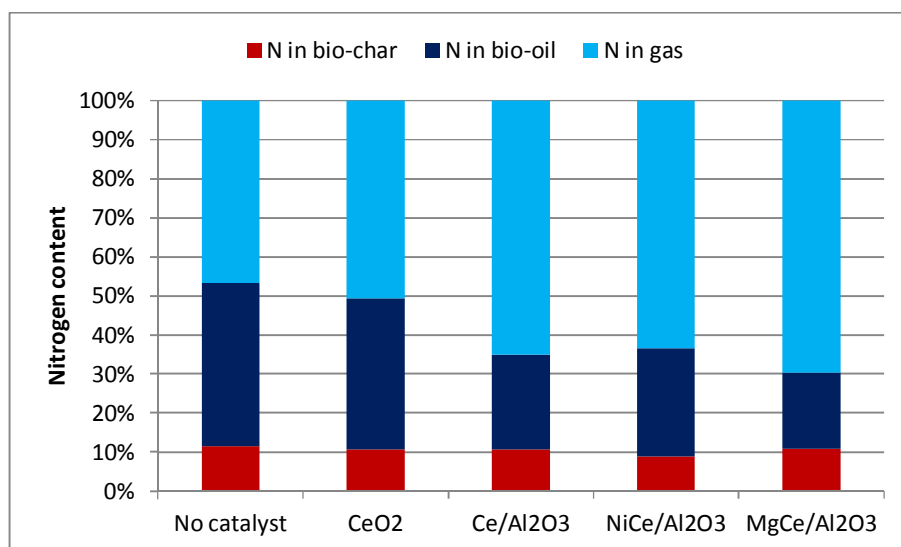


ACCEPTED

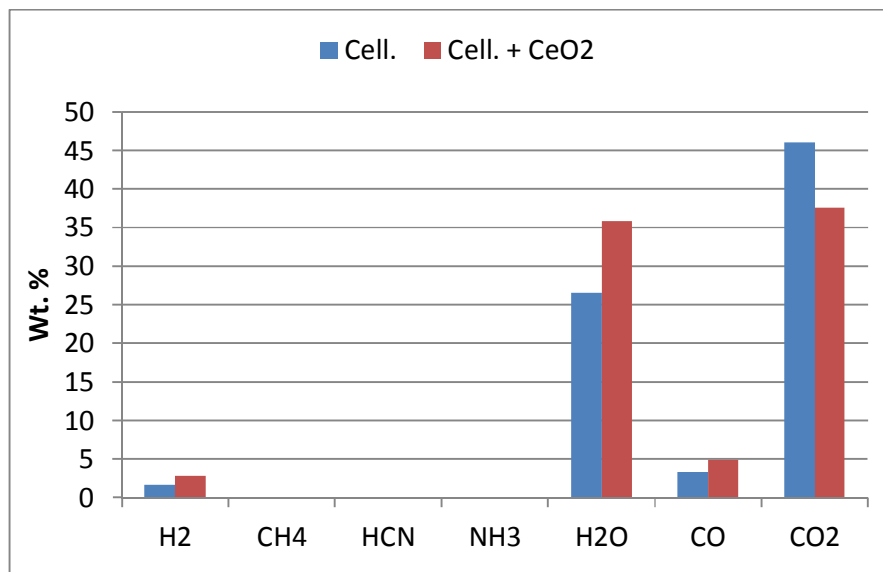




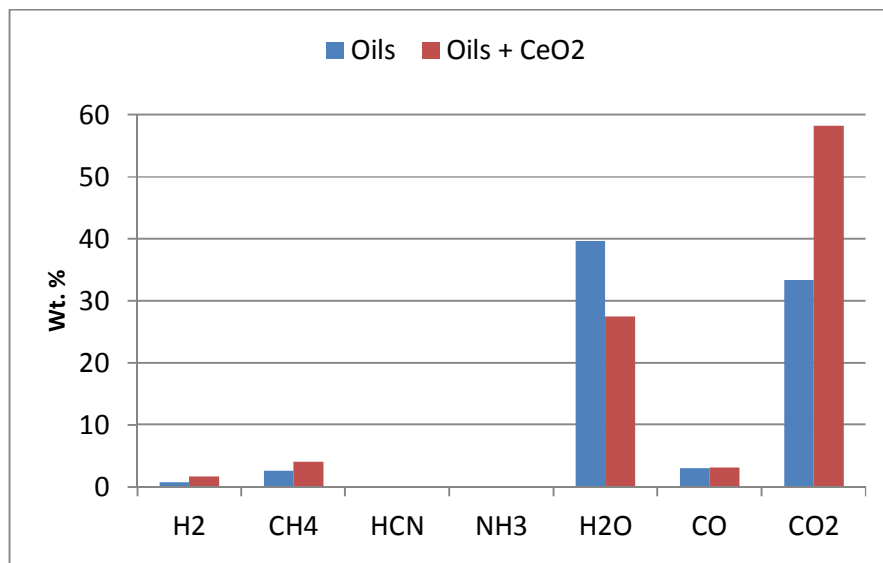
ACCEPTED MANUSCRIPT



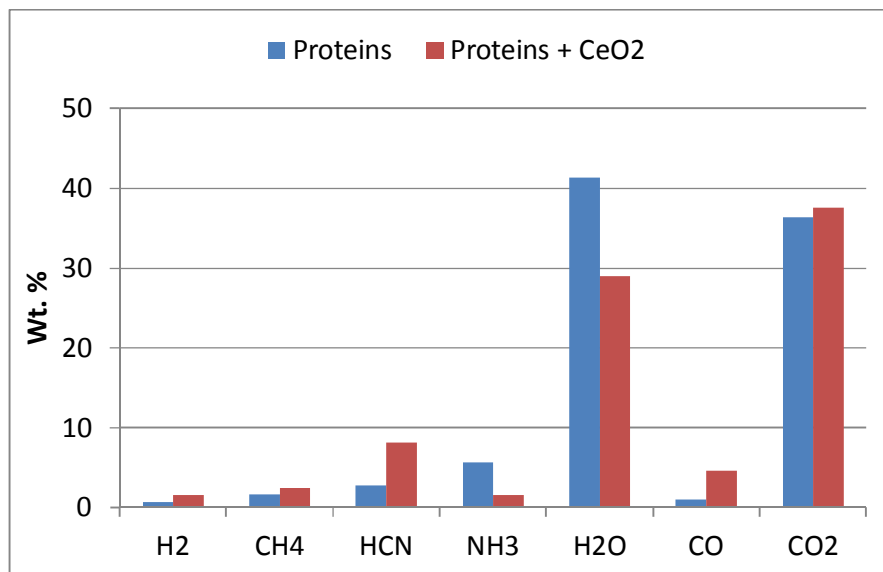
ACCEPTED MANUSCRIPT



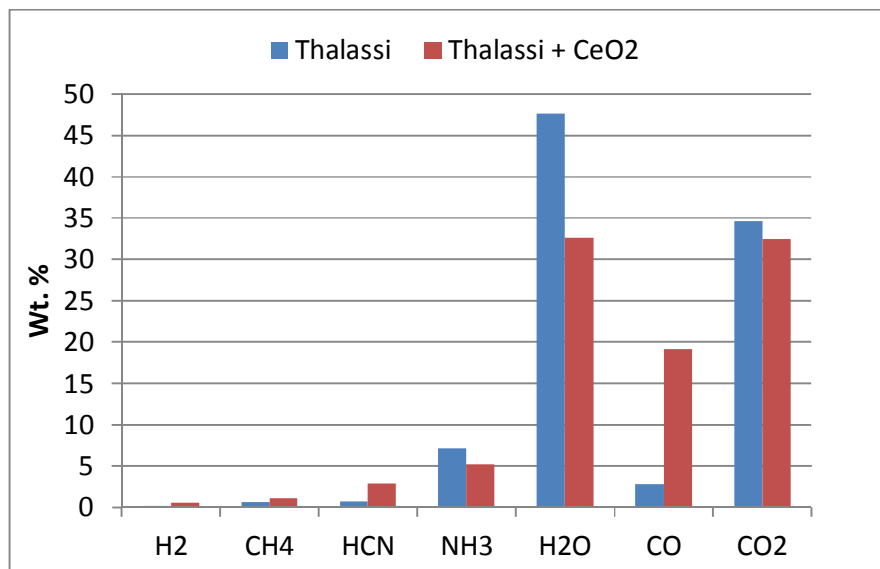
ACCEPTED MANUSCRIPT



ACCEPTED MANUSCRIPT



ACCEPTED MANUSCRIPT



ACCEPTED MANUSCRIPT

## Highlights

- *Thalassiosira weissflogi* and its model compounds were pyrolysed over ceria catalysts
- The highest liquid yield (25.8%) was obtained in presence of CeO<sub>2</sub> at 500°C
- Ceria catalysts increased aliphatics and decreased oxygenate compounds
- Dehydration and decarboxylation were the main deoxygenation reactions
- Ceria catalysts consistently reduced N-content in bio-oil

ACCEPTED MANUSCRIPT